

# Localized Corrosion of Mild Steel in H<sub>2</sub>S Containing Aqueous Environments—Case Studies and Common Mechanisms

Saba Navabzadeh Esmaeely<sup>†,\*</sup> and Srdjan Nešić<sup>\*\*</sup>

*The current study is aimed at proposing a common mechanism of localized corrosion of mild steel in H<sub>2</sub>S containing aqueous environments, by utilizing experimental findings reported in a number of studies from the open literature. It is hypothesized that a discontinuity in an iron sulfide corrosion product layer due to poor formation or a disruption results in initiation of localized corrosion. Then a galvanic coupling between the underlying steel and the conductive iron sulfide corrosion product layer leads to propagation of localized corrosion at an enhanced rate. This hypothesis was tested by using five different cases where localized corrosion was observed, which were all in support of the proposed mechanism. These were Case 1: a poorly formed mackinawite layer Case 2: a partially dissolved pyrrhotite layer Case 3: a disrupted pyrrhotite layer due to pyrite formation Case 4: a disrupted pyrrhotite layer due to presence of sand, and, finally, Case 5: a disrupted mackinawite layer due to interference by pyrite.*

KEY WORDS: localized corrosion, H<sub>2</sub>S, iron sulfide, mackinawite, pyrite, pyrrhotite

## INTRODUCTION

In aqueous H<sub>2</sub>S environments, localized corrosion of mild steel is one of the main concerns and has required a considerable effort to understand and ultimately prevent its occurrence. Localized corrosion often proceeds at a high rate at locations where the corrosion product layer is incomplete or damaged.<sup>1-2</sup> One of the complicating factors involving aqueous H<sub>2</sub>S corrosion of mild steel is the role of different iron sulfides<sup>3-9</sup> that could form as a corrosion product layer with distinct physicochemical and electrical properties.<sup>10-15</sup> The iron sulfide corrosion product layer's thermodynamics and properties have been investigated and reported in details in prior publications.<sup>16-21</sup> The electrochemical reactions involved in the corrosion process may be accelerated through a galvanic effect due to the additional cathodic surface area that is provided by the conductive iron sulfide corrosion product layer.<sup>17,21-25</sup>

Based on the general understanding described in the literature, the main reasons for localized corrosion in conductive aqueous H<sub>2</sub>S solutions can be ascribed to three reasons: the formation of elemental sulfur,<sup>26-29</sup> partial formation/failure of the iron sulfide corrosion product layer,<sup>19,30</sup> and formation of multiple iron sulfide polymorphs in a corrosion product layer, leading to nonuniform electrical conductivity.<sup>31-33</sup> Although most of the individual studies found in the open literature<sup>19,26-33</sup> present findings that appear to be valid in isolation, none of them put forward a common mechanism that can explain localized corrosion beyond their specific conditions. Even the first questions that one faces dealing with H<sub>2</sub>S corrosion: which iron sulfide is the most detrimental when it comes to localized corrosion, is in dispute. Therefore, the present study attempts to

bridge these gaps and propose an overarching explanation of mild steel localized corrosion in aqueous H<sub>2</sub>S solutions and the role of different iron sulfides.

In the current study we hypothesize the following:

- a condition leading to poor formation or disruption of the iron sulfide corrosion product layer results in initiation of localized corrosion;
- localized corrosion then propagates at that discontinuity in the corrosion product layer via galvanic coupling between the underlying steel and the conductive iron sulfide layer.

As obvious as this hypothesis may seem, which has been an accepted mechanism for corrosion resistance alloys and stainless steel materials, it was not previously proposed in any of the H<sub>2</sub>S studies found in the open literature, covering a broad range of scenarios in which localized corrosion was observed. In order to verify this hypothesis, the current study examines five rather different conditions of steel corroding in aqueous H<sub>2</sub>S solutions in which localized corrosion was observed.<sup>18-19,31-32,34</sup>

The criteria used to select these representative cases were as follows: the experimental study had to be executed under well controlled conditions; the study had to be long enough so that localized corrosion could develop and be unambiguously detected; and proper surface analysis was executed enabling the phase identifications and pit depth measurements.

Each of the five selected conditions is described below in some detail, followed by a discussion explaining the probable localized corrosion mechanism and how it is consistent with the proposed hypothesis. These cases include the following:

- Case 1: a poorly formed mackinawite layer;
- Case 2: a partially dissolved pyrrhotite layer;

Submitted for publication: January 20, 2019. Revised and accepted: April 15, 2019. Preprint available online: April 15, 2019, <https://doi.org/10.5006/3164>.

<sup>†</sup> Corresponding author. E-mail: [sn294410@ohio.edu](mailto:sn294410@ohio.edu).

\* The Fontana Corrosion Center, Department of Material Science and Engineering, The Ohio State University, Columbus, Ohio 43202.

\*\* Institute for Corrosion and Multiphase Technology, Department of Chemical and Biomolecular Engineering, Ohio University, Athens, Ohio 45701.

- Case 3: a disrupted pyrrhotite layer due to pyrite formation;
- Case 4: a discontinuous pyrrhotite layer due to presence of sand,
- Case 5: a disrupted mackinawite layer due to the interference by pyrite.

## CASE ANALYSIS AND DISCUSSION

### 2.1 | Case 1—A Poorly Formed Mackinawite Layer

It has been reported that a thin iron sulfide corrosion product layer—mackinawite—is formed on mild steel exposed to aqueous  $H_2S/CO_2$  environments, which typically decreases the uniform corrosion rate.<sup>8,35-39</sup> However, when very small (trace) amounts of  $H_2S$  are present in  $CO_2$ , this leads to formation of a partially protective mackinawite layer, which results in localized corrosion.<sup>19,30,40-41</sup> For example, mild steel underwent localized corrosion when exposed to an aqueous solution saturated with ~100 ppm<sub>v</sub>  $H_2S$  in a  $CO_2$  gas phase, at atmospheric conditions, where the bulk solution was undersaturated with respect to both mackinawite and iron carbonate and trace amounts of dissolved oxygen were present (in the ppb range).<sup>19</sup> However, no localized corrosion occurred when  $H_2S/CO_2$  was either larger than 100 ppm<sub>v</sub> or in the absence of  $H_2S$  and trace amounts of oxygen (Figure 1).

Mackinawite is the least thermodynamically stable iron sulfide with the fastest kinetics of formation. Therefore it is always found as the initial corrosion product; it eventually

transforms to other more stable forms of iron sulfides, such as pyrrhotite and pyrite.<sup>42</sup> It has been reported that mackinawite usually forms as a series of thin layers parallel to the steel surface, consistent with its two dimensional/planar molecular structure.<sup>5,43</sup> This leads to anisotropic electronic conductivity of mackinawite with much higher conductivity in the planar direction.<sup>44-45</sup> When a protective mackinawite layer forms on the surface of the steel, it leads to retardation of the mass transfer of the species involved in the corrosion process ( $Fe^{2+}$  away from the surface and  $H^+$  towards the surface).

Under a poorly formed mackinawite layer, localized corrosion initiates as a result of discontinuities in the layer. This allows the corrosive species such as  $H^+$ , to reach the mild steel surface and be reduced there, while  $Fe^{2+}$  leaves the steel lattice more readily and diffuses away, allowing the corrosion process to proceed unimpeded at these locations. Given that the pitting penetration rates reported in above mentioned study (Figure 1), were significantly higher than the bare steel uniform corrosion rate at the same conditions, one can conclude that this is due to a galvanic coupling between the poorly protected mild steel and the conductive mackinawite layer.

### 2.2 | Case 2—A Partially Dissolved Pyrrhotite Layer

Pyrrhotite is one of the most abundant iron sulfides found in the Earth's crust,<sup>14,46-48</sup> which is also a corrosion product commonly formed in aqueous  $H_2S$  corrosion of mild steel. Pyrrhotite ( $Fe_{(1-x)}S$  ( $x = 0-0.2$ ))<sup>47,49-52</sup> is an iron-deficient iron sulfide, with a

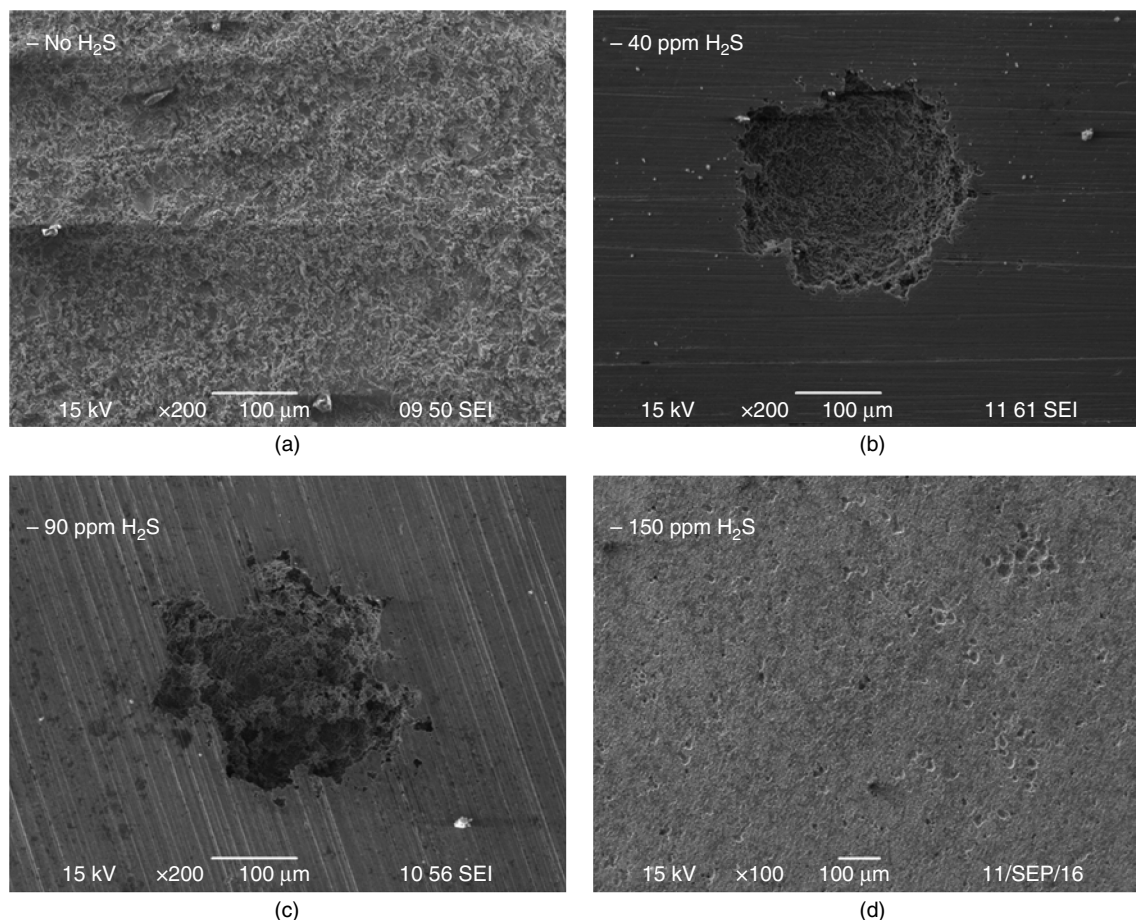


**FIGURE 1.** X65 specimens (a) no  $H_2S$ , (b) 40 ppm  $H_2S$ , (c) 90 ppm  $H_2S$  (d) 150 ppm  $H_2S$  exposed to an aqueous solution in  $CO_2$  at 30°C and pH 5.0, 1 wt% NaCl, 6 d exposure.<sup>21</sup>

monoclinic or hexagonal crystalline structure, depending on its iron deficiency. Hexagonal stoichiometric pyrrhotite is known as troilite. Pyrrhotite is a p-type semiconductor<sup>10-12</sup> and given its more positive open circuit potential versus mild steel, there is a possibility of galvanic coupling.<sup>53-55</sup> Additionally, pyrrhotite is electroactive<sup>56-58</sup> with a similar electroactivity as mild steel, when it comes to  $H^+$  or  $H_2S$  reduction.<sup>17</sup> When conditions are such that pyrrhotite forms as a dense uniform corrosion product layer that is well attached to the steel surface, it offers some protection to the steel underneath, via retardation of the anodic reaction due to surface blockage.<sup>27</sup> Being a semiconductive layer, pyrrhotite enables the corrosive species such as  $H^+$  and/or  $H_2S$  to be reduced at the outer surface of the layer, without needing to diffuse all the way to the steel surface. Under such conditions, the rate determining step is the rate of mass transfer of ferrous ions produced by the iron oxidation/dissolution away from the surface, rather than the mass transfer rate of the cathodic species  $H^+$  and/or  $H_2S$ . However, a pyrrhotite layer can also have a detrimental role when it is not dense or uniform (similar to what was described above for mackinawite).

In a previously published study,<sup>18</sup> it was shown that mild steel specimens, with a preformed nonprotective pyrrhotite layer, experienced localized attack when exposed to aqueous  $CO_2$  or aqueous  $CO_2/H_2S$  solutions. In those experiments, the steel was pretreated at high-temperature in a sulfur-containing oil in order to form a layer of pyrrhotite via direct sulfidation. The pretreated specimens were then exposed to a range of aqueous  $CO_2$  and  $H_2S$  corrosion environments. In an aqueous  $CO_2$  solution, the pyrrhotite layer underwent partial dissolution whereas in a mixed  $CO_2/H_2S$  solution, the preformed pyrrhotite layer partially transformed to troilite, with some mackinawite formation at the steel surface. Under both conditions, initiation of localized corrosion was observed:  $Fe^{2+}$  dissolution from the steel lattice occurred more readily at the sites where the pyrrhotite layer dissolved or transformed into troilite.

It was reported that the pitting penetration rate increased significantly when a more conductive electrolyte was used, approximately 4 mm/y in a solution without salt, and 14 mm/y in a 1 wt% NaCl solution (see Figure 2). The semiconductive pyrrhotite layer surrounding the pit led to galvanically driven localized corrosion more so in a more conductive electrolyte.<sup>18</sup>

According to the main hypothesis proposed in the present study, the localized attack was initiated as a result of partial dissolution/transformation of the preformed pyrrhotite layer.<sup>18</sup> Subsequently, the localized corrosion attack propagated at a high

rate due to the galvanic coupling between the exposed mild steel surface and the surrounding conductive pyrrhotite layer.<sup>21</sup>

### 2.3 | Case 3-A Disrupted Pyrrhotite Layer Due to Pyrite Formation

Formation of iron sulfide corrosion products is a transient process; the initial product is mackinawite, having the fastest kinetics of formation. The corrosion product layer ultimately evolves to a more stable layer containing thermodynamically stable species such as pyrrhotite or pyrite if the environmental condition allows it.<sup>3,8,34,39,59-63</sup>

Localized corrosion associated with a pyrrhotite or pyrrhotite/pyrite mixed corrosion product layer has been observed across a wide range of experimental conditions. Gao, et al.,<sup>34</sup> conducted autoclave experiments at constant aqueous  $H_2S$  concentration (0.00385 mol/L, where  $pH_2S$  was in the range of 0.1 bar to 0.18 bar) at different temperatures (80°C to 200°C). They reported localized corrosion under pyrrhotite/pyrite layers. In another study,<sup>20</sup> conducted at high-temperature (120°C) and high partial pressures of  $H_2S$  (0.1 bar to 2 bar), similar results were observed by the same authors. Under these two rather distinct sets of conditions, one at a lower temperature (120°C)<sup>20</sup> with 1 bar  $pH_2S$  and the other at a higher temperature (200°C) at lower  $pH_2S$  (0.18 bar), localized corrosion occurred only when a mixed pyrrhotite/pyrite layer was observed. What seemed to be common between these two cases was formation of pyrite in a matrix of pyrrhotite. This is consistent with the hypothesis where disruption of pyrrhotite corrosion product layer by pyrite led to initiation of localized corrosion.

The disruption of a pyrrhotite layer by pyrite nucleation has been investigated in mineralogy in great depth,<sup>64-69</sup> where disruptive nucleation of different phases in a "parent" phase (here pyrite within the pyrrhotite layer) has been well established. Although there is a grave difference in the duration of processes, the well understood transformation process in geological systems could be used to better understand such phenomena in a less established field such as aqueous  $H_2S$  corrosion of mild steel. As the pyrite phase nucleates in the parent pyrrhotite phase, microcracks form; this results in a disruption in the pyrrhotite layer depending on the pathway that this process follows. Pyrrhotite transformation to pyrite has been postulated to take place via one of three possible pathways:

- (a) It could happen through formation of an intermediary phase, marcasite by solid-state reaction, where,

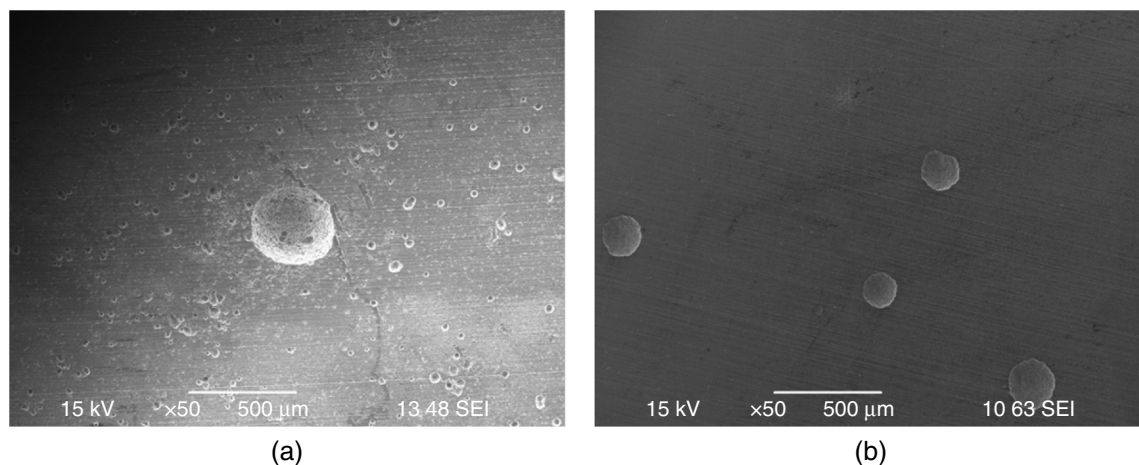


FIGURE 2. Pretreated specimens after exposure to aqueous  $CO_2$  solution at 30°C and pH 4.0 (a) 1 wt% NaCl, (b) no NaCl.<sup>21</sup>

marcasite crystals follow the preferred orientation-hexagonal symmetry of the parent pyrrhotite; this transformation results in a volume reduction of iron sulfide by approximately 30% and large micron-size cracks; this is followed by solidstate transformation of marcasite to pyrite with further formation of smaller cracks, due to additional volume reduction of approximately 3%.<sup>66</sup>

- (b) The second pathway is similar, except that the transformation of pyrrhotite to marcasite is by dissolution/precipitation with a random orientation for the crystals; this also results in the formation of micron-size cracks.
- (c) Pyrrhotite is directly transformed into pyrite by oxidative dissolution of pyrrhotite, followed by direct precipitation of pyrite, with the final outcome being a porous layer with very fine cracks and lower porosity.<sup>64-65</sup>

These iron sulfide phase transformations occurring in a corrosion product layer play a significant role in localized

corrosion initiation. It explains why in Gao's<sup>20</sup> experiments pyrite formation within a pyrrhotite layer led to disruption followed by galvanic attack stemming from the conductive nature of the pyrrhotite/pyrite layer in a conductive electrolyte. This resulted in propagation of localized corrosion.

#### 2.4 | Case 4-A Disrupted Pyrrhotite Layer Due to Presence of Sand

Solid deposits containing various iron sulfide particles mixed with sand and organic particles are encountered in the field leading to localized corrosion.<sup>70-72</sup> Kvarekval and Svenningsen<sup>32</sup> reported localized corrosion under pyrrhotite/troilite deposit layers exposed to aqueous solutions at room temperature under high-pressure conditions (10 bar H<sub>2</sub>S and 10 bar CO<sub>2</sub>). In their study, the cross section images of tested specimens showed that the corrosion product layers under the pyrrhotite/troilite particles had noticeable defects with the

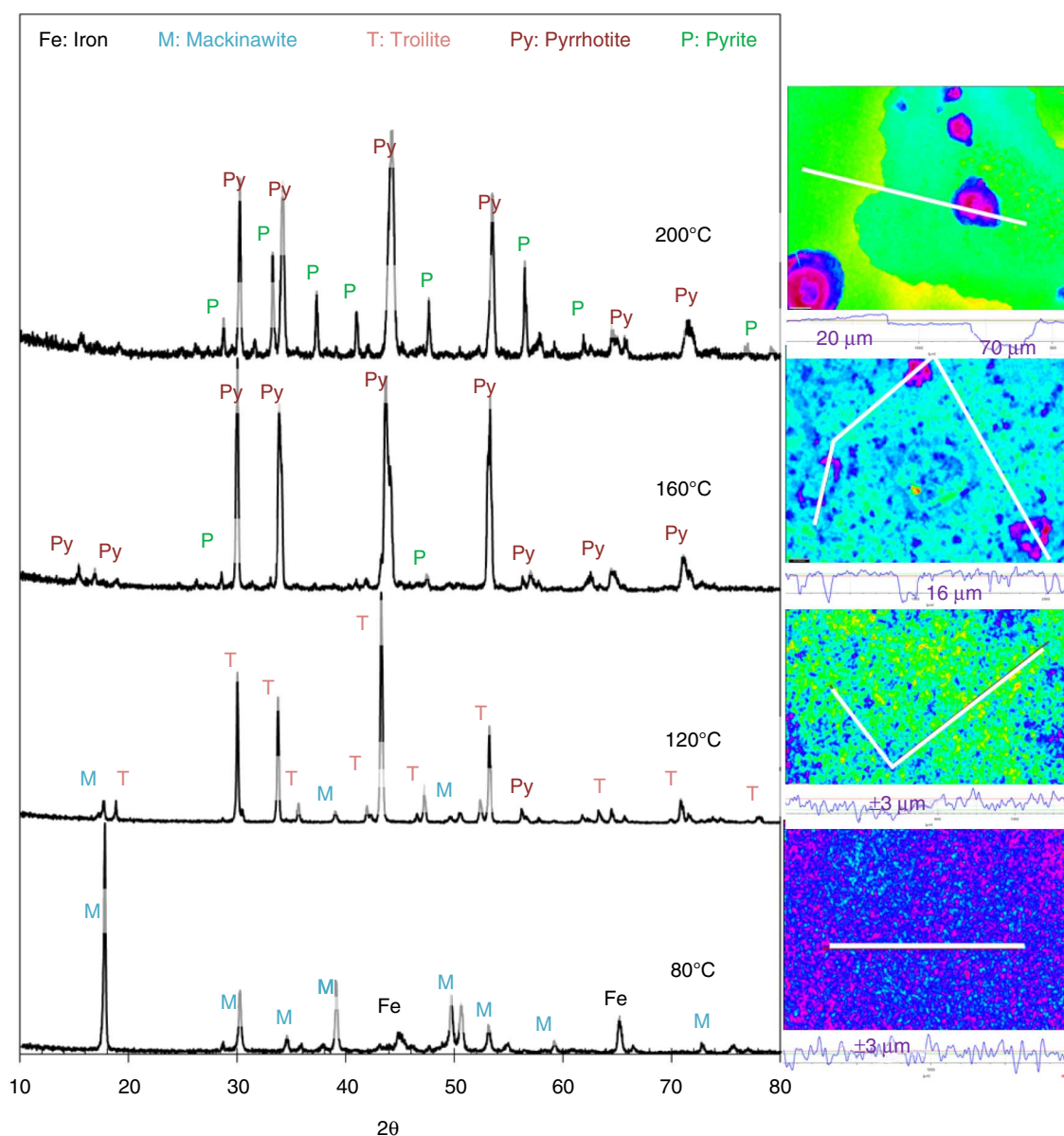


**FIGURE 3.** X-ray diffraction (XRD) and profilometry analysis of the specimen postexposure to a constant H<sub>2</sub>S concentration of 0.00385 mol/L at different temperatures, initial pH 4.0, and 4 d exposure.<sup>34</sup>

deposited particles penetrating into corrosion product layer, thereby disrupting it. The authors also reported localized attack under a mixed pyrrhotite/troilite layer including sand when exposed to similar conditions. In a recent study, corrosion of mild steel under deposit layers containing pyrrhotite, pyrite, and sand particles was investigated by Esmaeely.<sup>21</sup> In different

experiments the pyrrhotite particles were mixed with pyrite particles or sand. In aqueous CO<sub>2</sub> conditions at atmospheric pressure, localized corrosion was not observed under deposits of very fine pyrrhotite particles. However, localized corrosion was observed under layers containing larger pyrrhotite particles and under a mixed pyrrhotite/pyrite or pyrrhotite/sand layer.

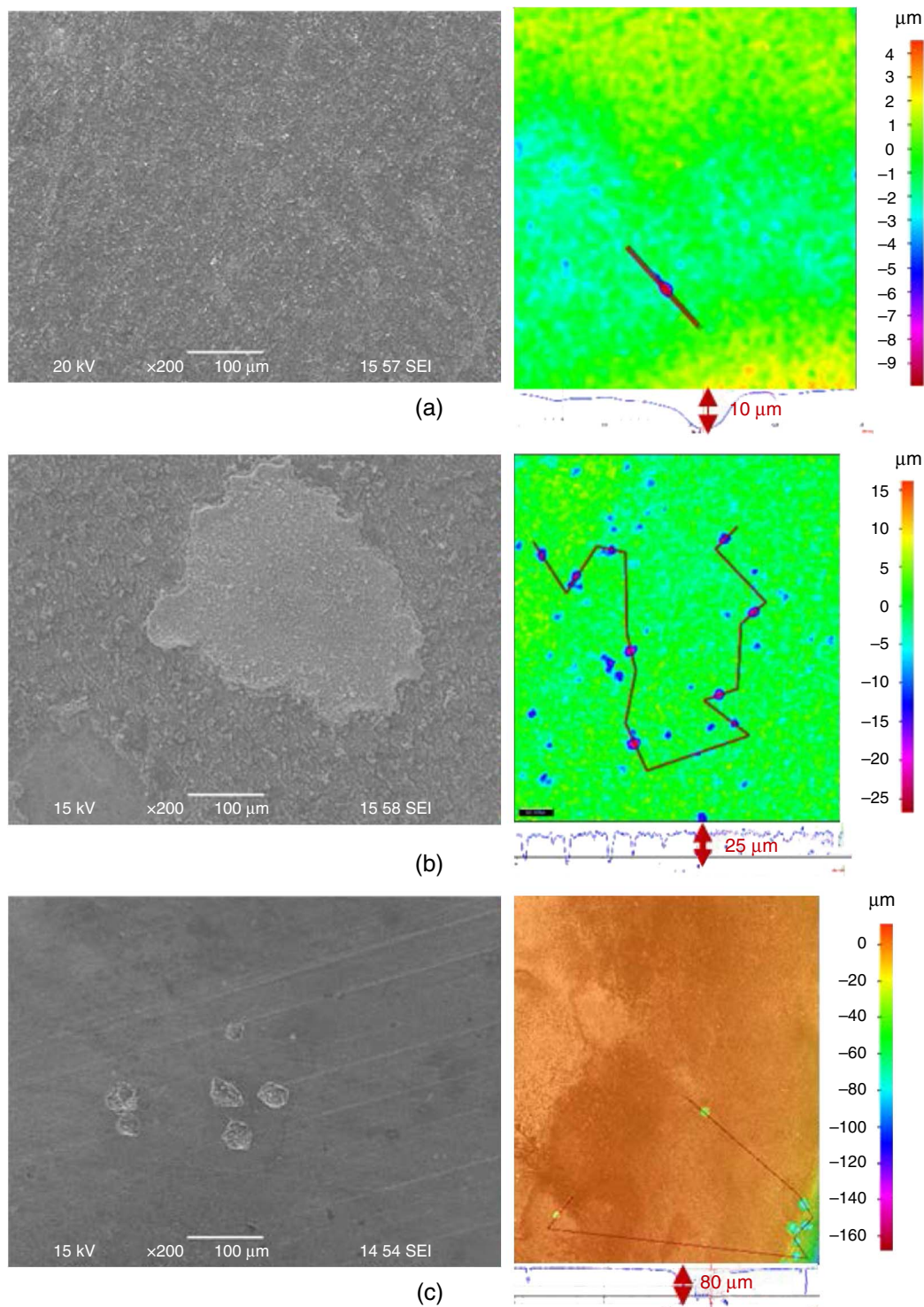


**FIGURE 4.** X65 scanning electron microscope (SEM) and profilometry image under (a) 0.25 g/cm<sup>2</sup> pyrrhotite (b) 0.125 g/cm<sup>2</sup> pyrrhotite + 0.125 g/cm<sup>2</sup> pyrite, and (c) 0.125 g/cm<sup>2</sup> pyrrhotite + 0.125 g/cm<sup>2</sup> sand in aqueous CO<sub>2</sub> solutions at pH 4.0, 30°C, 1 wt% NaCl, (particle size 400 µm to 1,000 µm).<sup>21</sup>

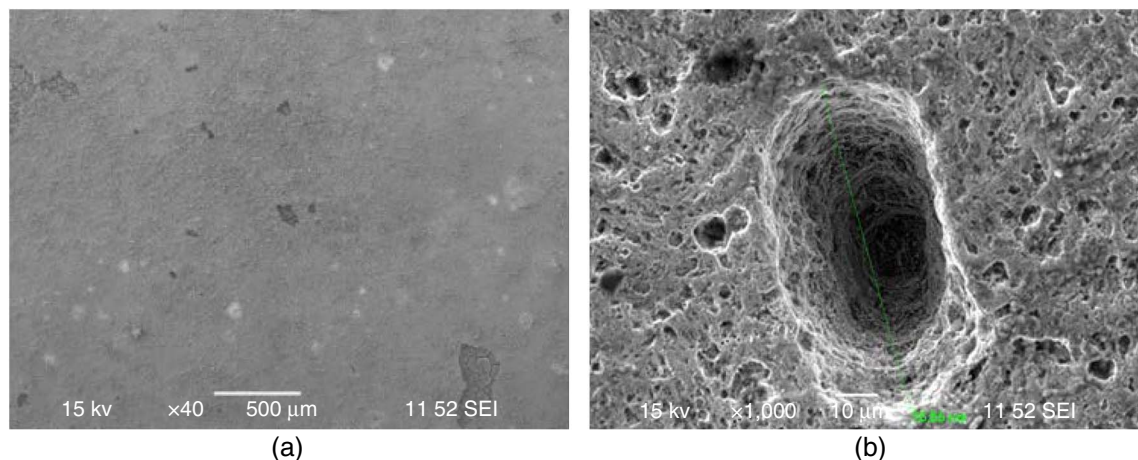


**FIGURE 5.** X65 under 2 mm thick pyrite deposit, (a) with the corrosion product layer (b) without the corrosion product layer exposed to an aqueous solution sparged with  $p_{H_2S} = 0.1$  bar at 25°C, 1 wt% NaCl, Initial pH 4.0.<sup>16</sup>

Compared to a pure pyrrhotite layer, the intensity of localized attack was higher when pyrrhotite was mixed with pyrite and highest when it was mixed with sand (Figure 4).

In the experiments reported above, the mixed layer was used in an attempt to simulate the effect of a disrupted pyrrhotite layer. The experimental results showed that localized corrosion initiated as a result of that discontinuity/disruption and propagated due to the galvanic coupling of the steel surface and the semiconductive pyrrhotite containing deposit layer, what is consistent with the hypothesis proposed above.<sup>21</sup>

### 2.5 | Case 5—A Disrupted Crystalline Mackinawite Layer Due to Interference by Pyrite

In a study conducted by Ning,<sup>16</sup> localized corrosion was reported under a pyrite deposit layer placed on a mild steel specimen surface exposed to an aqueous  $H_2S$  solution. In the absence of pyrite particles these conditions lead to formation of a protective mackinawite layer. It was suggested by Ning<sup>16</sup> that pyrite formation enhances the mackinawite layer's conductivity in the direction perpendicular to the steel surface which led to a more effective galvanic coupling. Ultimately, this resulted in localized corrosion according to Ning<sup>16</sup> (Figure 5).

However, the proposed increase in conductivity of the mackinawite layer does not seem to fully explain the occurrence of localized corrosion, as reported by Ning.<sup>16</sup> A uniform mackinawite layer (with an improved conductivity) would lead to uniform corrosion, possibly at a higher rate due to a galvanic coupling. For localized corrosion to happen there needs to be a local disruption of the mackinawite layer, where corrosion happens unimpeded at a higher rate. This amounts to an initiation of localized attack. Subsequently, the attack propagates much faster because of galvanic coupling of the exposed steel and the mixed iron sulfide corrosion product layer.

## DISCUSSION

Based on the proposed mechanism and the evidence in the open literature, it may be useful for practical applications to identify some of the *root causes* of localized corrosion of mild steel in aqueous  $H_2S$  solutions.<sup>(1)</sup>

- **Trace amounts of  $H_2S$  in the presence of  $CO_2$ ,** commonly known as marginally sour conditions. Under these conditions, the mackinawite layer that forms is not continuous, which results in localized corrosion initiation. The propagation of localized attack is aggravated due to galvanic coupling between the mild steel and the conductive mackinawite layer.
- **Water chemistry changes leading to dissolution of the iron sulfide corrosion product layer.** Changes in solubility of iron sulfides are brought about by changes in operating conditions such as pH, temperature, partial pressure of  $H_2S$ , salt concentration, etc. Under those conditions in which the solubility of iron sulfides decreases, the layer undergoes dissolution, which is a nonuniform process; this leads to initiation of localized corrosion at locations that dissolve first, followed by propagation due to galvanic coupling.
- **Conditions leading to transformations from one form of iron sulfide to another.** Some of these transformations are a result of differences in thermodynamic stability and kinetics of formation of various iron sulfides (such as, for example, transformation of mackinawite to troilite and pyrrhotite). Other transformations are caused by water chemistry changes either in the bulk solution or within the corrosion product layer. The best example is the transformation of pyrrhotite into pyrite, which can lead to disruptions in the layer due to their different crystal structures, followed by localized corrosion propagation.
- **Presence of deposits.** Solid deposits are a common occurrence in oil and gas transportation lines due to settling at low flow velocities. They can include produced sand, particles formed by spalling of the corrosion product layer such as iron carbonate and iron sulfides, scale particles such as calcium carbonate, barium sulfate, etc., and organic matter such as asphaltenes and waxes. The presence of these deposits interferes with the iron sulfide corrosion product formation which results in a noncontinuous layer. This may lead to localized corrosion initiation and propagation due to the galvanic effect.
- **Chlorides.** The  $Cl^-$  ion is commonly referred to as one of the main causes that leads to localized corrosion for a broad range of metals and alloys in a wide variety of environments. Although this is well documented and

<sup>(1)</sup> The exception that is not included in the current discussion is localized corrosion due to the presence of elemental sulfur, which appears to have a different mechanism.

explained for the case of passive metals, there is much less clarity when it comes to the direct effect of  $\text{Cl}^-$  on localized corrosion of mild steel. Although some circumstantial evidence exists linking the presence of  $\text{Cl}^-$  with occurrence of localized attack, systematic studies explaining the mechanisms are lacking. What seems to be the case is that elevated  $\text{Cl}^-$  concentration increases the solubility of the protective corrosion product layers such as iron carbonate<sup>73</sup> and possibly iron sulfides. This may lead to partial dissolution of the protective layer and initiation of localized corrosion described above. Furthermore, the presence of  $\text{Cl}^-$  increases the conductivity of the aqueous solution, which enhances the galvanic coupling and the rate of localized attack propagation.

## CONCLUSIONS

> It was shown that the localized corrosion observed under different conditions, discussed in the present study, seems to share a common mechanism. Whenever an iron sulfide corrosion product layer did not form uniformly or was disrupted, this led to a discontinuity that resulted in initiation of localized corrosion. Localized corrosion then propagated at that discontinuity via galvanic coupling between the underlying steel and the conductive iron sulfide corrosion product layer around it.

## ACKNOWLEDGMENTS

The authors acknowledge the financial support from a joint industry project including BP, Champion Technologies, Chevron, ConocoPhillips, DNV GL, ENI S.p.A., ExxonMobil, Hess, Multi-Chem, NALCO Energy Services, Occidental Petroleum Co., Petrobras, PETRONAS, PTT, Saudi Aramco, Inpex Corporation, SINOPEC, TOTAL, TransCanada, WGIM, and Shell. The authors would like to express their appreciation to Dr. Bert Pots, Dr. Bruce Brown, Dr. Michel Bonis, and Mr. Michael Joosten for their contributions to this study.

## References

- S. Nescic, "Carbon Dioxide Corrosion of Mild Steel," *Uhlig's Corrosion Handbook*, 3rd ed., ed. W. Revie (Hoboken, NJ: John Wiley and Sons Inc., 2011), p. 229.
- S. Nescic, W. Sun, "Acid Gas Corrosion," *Shrier's Corrosion*, 2nd ed., ed. J.A. Richardson (New York, NY: Elsevier, 2010), p. 1270.
- F. Shi, L. Zhang, J. Yang, M. Lu, J. Ding, H. Li, *Corros. Sci.* 102 (2016): p. 103-113.
- J. Ning, Y. Zheng, B. Brown, D. Young, S. Nescic, *Corrosion* 71 (2015): p. 945-960.
- D.W. Shoesmith, P. Taylor, M. Grant Bailey, D.G. Owen, *J. Electrochem. Soc.* 127 (1980): p. 1007-1015.
- L.G. Benning, R.T. Wilkin, H.L. Barnes, *Chem. Geol.* 167 (2000): p. 25-51.
- W.H. Thomason, "Formation Rates of Protective Iron Sulfide Films on Mild Steel in  $\text{H}_2\text{S}$ -Saturated Brine as a Function of Temperature," CORROSION 1978, paper no. 41 (Houston, TX: NACE, 1978).
- F.H. Meyer, O.L. Riggs, R. L. McGlasson, J. D. Sudbury, *Corrosion* 14 (1957): p. 69-75.
- W. Zhao, Y. Zou, K. Matsuda, Z. Zou, *Corros. Sci.* 102 (2016): p. 455-468.
- D.F. Pridmore, R. Shuey, *Am. Mineral.* 61 (1976): p. 248-259.
- C.I. Pearce, R. Patrick, D. Vaughan, *Rev. Mineral. Geochem.* 61 (2006): p. 127-180.
- R. Schieck, A. Hartmann, S. Fiechter, R. Konenkamp, H. Wetzler, *J. Mater. Res.* 5 (2000): p. 1567-1572.
- P.K. Abraitis, R. Patrick, D.J. Vaughan, *Int. J. Miner. Process.* 74 (2004): p. 41-59.
- D.J. Vaughan, "Mineral Chemistry of Metal Sulfides" (Cambridge University Press, 1978), p. 17-117, ISBN 10: 0521214890.
- A.R. Lennie, K. England, D.J. Vaughan, *Am. Mineral.* 80 (1995): p. 960-967.
- J. Ning, "The Role of Iron Sulfide Polymorphism in Localized Corrosion of Mild Steel" (Ph.D. diss., Ohio University, 2016).
- S.N. Esmaeely, S. Nescic, *J. Electrochem. Soc.* 164 (2017): p. C664-C670.
- S.N. Esmaeely, G. Bota, B. Brown, S. Nescic, *Corrosion* 74 (2018): p. 37-49.
- S.N. Esmaeely, W. Zhang, B. Brown, M. Singer, S. Nescic, *Corrosion* 73 (2017): p. 1098-1106.
- S. Gao, "Thermodynamics and Kinetics of Hydrogen Sulfide Corrosion of Mild Steel at Elevated Temperatures" (Ph.D. diss., Ohio University, 2018).
- N. S. Esmaeely, "Galvanic Localized Corrosion of Mild Steel under Iron Sulfide Corrosion Product Layers" (Ph.D. diss., Ohio University, 2018).
- B.W. Bolmer, *Corrosion* 21 (1965): p. 69-75.
- S.P. Ewing, *Corrosion* 11 (1955): p. 51-55.
- Y. Zheng, B. Brown, S. Nescic, *Corrosion* 70 (2014): p. 351-365.
- M. Tjelta, J. Kvarekval, "Electrochemistry of Iron Sulfide and its Galvanic Coupling to Carbon Steel in Sour Aqueous Solution," CORROSION 2016, paper no. 7478 (Houston, TX: NACE, 2016).
- H. Fang, "Investigation of Localized Corrosion of Carbon Steel in  $\text{H}_2\text{S}$  Environments" (Ph.D. diss., Ohio University, 2012).
- D. MacDonald, B. Robert, J.B. Hyne, *Corros. Sci.* 18 (1978): p. 411-425.
- G. Schmitt, *Corrosion* 47 (1991): p. 285-308.
- N. Yaakob, "Top of the Line Corrosion in  $\text{CO}_2/\text{H}_2\text{S}$  Environments" (Ph.D. diss., Ohio University, 2015).
- N. Yaakob, F. Farelis, M. Singer, S. Nescic, D. Young, "Localized Top of the Line Corrosion in Marginally Sour Environments," CORROSION 2016, paper no. 7695 (Houston, TX: NACE, 2016).
- J. Ning, Y. Zheng, B. Brown, D. Young, S. Nescic, *Corrosion* 73 (2017): p. 155-168.
- J. Kvarekval, G. Svenningsen, "Effect of Iron Sulfide Deposits on Sour Corrosion of Carbon Steel," CORROSION 2016, paper no. 7313 (Houston, TX: NACE, 2016).
- O. Yopez, N. Obeyesekere, J. Wylde, "Study of Sour Corrosion Mechanism under Controlled pH," CORROSION 2016, paper no. 7795 (Houston, TX: NACE, 2016).
- S. Gao, P. Jin, B. Bruce, D. Young, S. Nescic, *Corrosion* 73 (2017): p. 915-926.
- J. Lee, "A Mechanistic Modeling of  $\text{CO}_2$  Corrosion of Mild Steel in the Presence of  $\text{H}_2\text{S}$ " (Ph.D. diss., Ohio University, 2004).
- S. Grousset, M. Bayle, A. Dauzeres, D. Crusset, V. Deydier, Y. Linard, P. Dillmann, F. Mercier-Bion, D. Neff, *Corros. Sci.* 112 (2016): p. 264-275.
- S.N. Smith, "A Proposed Mechanism for Corrosion in Slightly Sour Oil and Gas Production," CORROSION 1993 (Houston, TX: NACE, 1993).
- X.B. Huang, Z.F. Yin, H.L. Li, Z.Q. Bai, W.Z. Zhao, *Corros. Eng. Sci. Technol.* 47 (2012): p. 78-83.
- H. Ma, X. Cheng, G. Li, S. Chen, Z. Quan, S. Zhao, L. Niu, *Corros. Sci.* 42 (2000): p. 1669-1683.
- W. Zhang, B. Brown, D. Young, S. Nescic, M. Singer, "Factors Influencing Localized Corrosion of Mild Steel in Marginally Sour Environments," CORROSION 2018, paper no. 10984 (Houston, TX: NACE, 2018).
- W. Yan, B. Brown, "Investigation of the Threshold Level of  $\text{H}_2\text{S}$  for Pitting of Mild Steel in  $\text{CO}_2$  Aqueous Solutions," CORROSION 2018, paper no. 11472 (Houston, TX: NACE, 2018).
- M. Wolthers, L. Charlet, P.R. Van Der Linde, D. Rickard, C.H. Van Der Weijden, *Geochim. Cosmochim. Acta.* 69 (2005): p. 3469-3481.
- G. Genchev, K. Cox, T.H. Tran, A. Sarfraz, C. Bosch, M. Spiegel, A. Erbe, *Corros. Sci.* 98 (2015): p. 725-736.
- A. Devey, R. Grau-Crespo, N. De Leeuw, *J. Phys. Chem.* 112 (2008): p. 10960-10967.
- K.D. Kwon, K. Refson, S. Bone, R. Qiao, W. Yang, Z. Liu, G. Sposito, *Phys. Rev. B* 83 (2011): p. 064402.
- M.F. Cai, Z. Dang, Y.W. Chen, N. Belzile, *Chemosphere* 61 (2005): p. 659-667.
- N. Belzile, Y.W. Chen, M.F. Cai, Y. Li, *J. Geochem. Explor.* 84 (2004): p. 65-76.
- P.H. Tewari, G. Wallace, A.B. Campbell, "The Solubility of Iron Sulfides and their Role," in *Mass Transport in Girdler-Sulfide Heavy Water Plants*, Canadian Atomic Energy Commission, Report AECL5960, 1978.

49. J.S. Smith, J.D. Miller, *Br. Corros. J.* 10 (1975): p. 136-143.
50. A.V. Kuklinskii, Y.L. Mikhlin, G.L. Pashkov, V.F. Kargin, I.P. Asanov, *Russ. J. Electrochem.* 37 (2001): p. 1269-1276.
51. Y.L. Mikhlin, A.V. Kuklinskii, G.L. Pashkov, I.P. Asanov, *Russ. J. Electrochem.* 37 (2001): p. 1277-1282.
52. Y. Mikhlin, V. Varnek, I. Asanov, Y. Tomashevich, A. Okotrub, A. Livshits, G. Selyutin, G. Pashkov, *Phys. Chem. Chem. Phys.* 2 (2000): p. 4393-4398.
53. C.M.V.B. Almeida, B.F. Giannetti, *J. Electrochem. Chem.* 553 (2003): p. 27-34.
54. K.K. Mishra, K. Osseo-Asare, *J. Electrochem. Soc.* 135 (1988): p. 2502-2509.
55. I.C. Hamilton, R. Woods, *J. Electrochem. Chem. Interf. Electrochem.* 118 (1981): p. 327-343.
56. P.D. Nicol, M.J. Scott, *J. South Afr. Inst. Min. Metall.* 79 (1979): p. 298-305.
57. E. Peters, H. Majima, *Can. Metall. Q.* 7 (1968): p. 111-117.
58. E. Peters, "The Electrochemistry of Sulfide Metals," *Trends in Electrochemistry*, eds. J.O. Bockris, D.A.J. Rand, B.J. Welch, (New York: Plenum Press, 1977), p. 267-290.
59. W. Davison, *Aquat. Sci.* 53 (1991): p. 309-329.
60. P. Bai, S. Zheng, H. Zhao, Y. Ding, J. Wu, C. Chen, *Corros. Sci.* 87 (2014): p. 397-406.
61. J. Morse, F. Millero, J. Cornwell, D. Rickard, *Earth Sci. Rev.* 24 (1978): p. 1-42.
62. R. Gee, Z.Y. Chen, *Corros. Sci.* 37 (1995): p. 2003-2011.
63. S. Gao, B. Brown, D. Young, M. Singer, *Corros. Sci.* 135 (2018): p. 167-176.
64. G. Qian, F. Xia, J. Brugger, W.M. Skinner, J. Bei, G. Chen, A. Pring, *Am. Mineral.* 96 (2011): p. 1878-1893.
65. J.B. Murowchick, *Econ. Geol.* 87 (1992): p. 1141-1152.
66. M.E. Fleet, *Can. Mineral.* 10 (1970): p. 225-231.
67. U.M. Graham, H. Ohmoto, *Geochim. Cosmochim. Acta* 58 (1994): p. 2187-2202.
68. J.W. Matthews, A.E. Blakeslee, *J. Cryst. Growth.* 32 (1974): p. 118-125.
69. R. Hull, J.C. Bean, D.J. Werder, R.E. Leibenguth, *Phys. Rev. B* 40 (1989): p. 1681-1684.
70. H.H. Abass, H.A. Nasr-El-Din, M.H. Ba-Taweel, *Soc. Pet. Eng.* (2002): SPE-77686-MS.
71. W. Sun, K. Chokshi, S. Nestic, "Iron Carbonate Scale Growth and the Effect of Inhibition in CO<sub>2</sub> Corrosion of Mild Steel," CORROSION 2005, paper no. 05285 (Houston, TX: NACE 2005).
72. J.L. Crolet, N. Thevenot, S. Nestic, *Corrosion* 54 (1998): p. 194-203.
73. W. Sun, S. Nestic, R.C. Woollam, *Corros. Sci.* 51 (2009): p. 1273-1276.